JURNAL KARTIKA KIMIA

J. Kartika Kimia, November 2022, 5, (2), 145-151
Journal homepage: http://jkk.unjani.ac.id/index.php/jkk
P-ISSN: 2655-1322 E-ISSN: 2655-0938

Docking and Dynamics Studies: Identifying the Binding Ability of Quercetin Analogs to the ADP-Ribose Phosphatase of SARS CoV-2

Arfan[1,*], Rahmat Muliadi[1], Rachma Malina[1], Nita Trinovitasari[1], Aiyi Asnawi[2]
[1]Faculty of Pharmacy, Universitas Halu Oleo, Kendari, Indonesia
[2]Faculty of Pharmacy, Universitas Bhakti Kencana, Bandung, Indonesia
*E-mail: arfan09@uho.ac.id

DOI: https://doi.org/10.26874/jkk.v5i2.143

Received: 12 Sept 2022, *Revised*: 18 Oct 2022, *Accepted*: 25 Oct 2022, O*nline*: 30 Nov 2022

Abstract

The SARS-CoV-2 coronavirus outbreak has resulted in severe pneumonia, even death (COVID-19). ADP-Ribose phosphatase (ADPR), a highly conserved macrodomain of this virus, was appropriate for viral RNA replication and transcription. According to studies, quercetin suppresses the main protease and 3-chymotrypsin and papain-like proteases, exhibiting antiviral efficacy against SARS CoV-2. However, quercetin analogs to ADPR have yet to be investigated. This study aims to obtain candidate compounds for ADPR based on binding energy, interaction mode, and binding stability using docking and molecular dynamics (MD) studies. The native ligand (AMP) has estimated binding energy based on docking results of -7.35 kcal/mol. Quercetin analogs, lig_C00013871 (Quercetin 3-(2"-galoylrutinoside), lig_C00006532 ([5',5']-Bisdihydroquercetin), and lig_C00013874 (Quercetin 3-(2G-(E)-p-coumaroylrutinoside) has more negative binding energy, with estimates of -9.43, -9.26, and -8.98 kcal/mol, respectively. These results align with binding energy estimates based on MM-GBSA of -14.76, -29.39, -34.90, and -42.79 kcal/mol for AMP, lig_C00006532, lig_C00013871, and lig_C00013874, respectively. According to the MD simulation, lig_C00006532 and lig_C00013874 will be more effective in stabilizing the ADPR complex. Finally, these two analogs are potential candidate compounds as ADPR inhibitors of SARS CoV-2.

Keywords: *ADPR, docking, MD, quercetin analogs, SARS CoV-2*

1 Introduction

SARS CoV-2, officially known as COVID-19, was a coronavirus that leads to severe acute respiratory syndrome and has become a health concern [1]. This disease infects various ages, from children to adults, with severe and even life-threatening symptoms [2]. Non-structural proteins (NSPs) and structural proteins, including spike glycoprotein, envelope, membrane, and nucleocapsid proteins, were encoded by the SARS CoV-2 positive-sense RNA [3]. The non-structural proteins, consisting of NSP1-10 and NSP12-16, are encoded by the viral RNA genome [4]. NSP3 was the most significant multidomain and transmembrane protein and played an essential role in the viral life cycle [5]. In addition, NSP3 also guides the viral genome to newly assembled replication complexes [6].

The multidomain SARS CoV-2 NSP3 enzyme contained 1.945 amino acids [7]. One of the critical functional domains in NSP3 was the ADP-ribose phosphatase (ADPR) domain which hydrolyzes the ADP-ribose modifications [8]. This enzyme is present in many viruses and very difficult to mutate [9].

A small molecule that binds strongly and inhibits ADP-ribose activity has substantial therapeutic value by reducing viral replication and increasing activation of the host IFN response [10,11]. A study by Jung et al. identified ten alternative ADRP inhibitors from 682 FDA-approved compounds [12]. In addition, Debnath et al. conducted a study to determine the activity of 113,687 natural compounds contained in the MolPort database [13]. These studies utilized a virtual screening approach to identify potential compounds with ADPR, but their stability through molecular dynamics simulations have yet to be determined.

Many studies have focused on the search for inhibitors of the SARS CoV-2 virus from natural compounds. However, no one has specifically identified the potential of quercetin as an ADPR inhibitor of SARS CoV-2. Quercetin has many pharmacological activities, including antioxidant, anti-inflammatory, antiviral, and immunoprotective [14]. Quercetin's antiviral activity against the influenza A virus (H1N1), hepatitis C virus, rhinovirus, herpes simplex virus, and dengue virus type 2 has been experimentally investigated in vitro and in vivo [15]. In addition, quercetin inhibited the main protease (Mpro), 3-chymotrypsin-like protease (3CLpro), and papain-like protease (PLpro) of SARS CoV-2. The production of pro-inflammatory cytokines that are imperative for the COVID-19 pulmonary phase, especially tumor necrosis factor, interleukin-1 (IL-1), IL-4, IL-6, and C-reactive protein, were also regulated by quercetin [14,16–18]. This study was designed to identify the potential of quercetin analogs as ADPR inhibitors from SARS CoV-2 and determine their stability by computational methods.

2 Method

2.1 Protein and Ligand Preparation

We selected the 3D structure of the ADPR of SARS CoV-2 from the RCSB website (PDB ID: 6W6Y) (https://www.rcsb.org/). This structure was selected based on Adenosine Monophosphate (AMP) as a native ligand. ADPR structure was then prepared by removing non-interacting ions and water molecules. In addition, Kollman charge and hydrogen atom were added using AutoDockTool 1.5.6 [19].

248 quercetin analogs were collected from Knapsack 3D (http://knapsack3d.sakura.ne.jp/). All molecules were prepared in the same program by adding hydrogen atoms and gasteiger charges, and the bonds in each molecule were arranged to rotate freely.

2.2 Molecular Docking Studies

The molecular docking simulations were run with iDock software [20]. The redocking process of the native ligand to the ADPR protein is a method to validate the docking protocol. Valid protocols are presented with a root mean square deviation (RMSD) value below 2 Å. The binding pocket was set by following the AMP coordinates with a grid area of 40 x 40 x 40 Å and 0.375 Å point spacing. The binding energies of all molecules were calculated, and their interactions were visualized with Discovery Studio Visualizer and PoseView (https://proteins.plus/).

2.3 Molecular Dynamics Studies

The molecular dynamics simulations of protein-ligand systems were run on GROMACS 2021.3 software [21]. Protein topology applies AMBER99SB-ILDN force field [22], and ligand topology applies General Amber force field with the help of Antechamber in AmberTool 2021 run in ACPYPE [23–25]. The solvation procedure employed a TIP3P water model at 310K and was neutralized by the addition of Na and Cl ions. The electrostatic force mimics the Particle Mesh Ewald method. The stability of the complex was determined by analyzing the root-mean-square deviation and fluctuations (RMSD and RMSF) of trajectory during the 50 ns simulation. The protein-ligand system's binding energies were determined by employing MM/GBSA methodology.

3 Result and Discussion

3.1 Docking Studies Analysis

Our aim in the redocking native ligand (AMP) to the ADPR was to validate the grid parameters before the quercetin analogs were docked to the target protein. We used the RMSD value of less than 2 Å as a valid parameter. Based on the results, the ADPR binding site had coordinates x-axis = 9.124, y-axis = -8.677 and z-axis = 16.22. The coordinates and grid parameters were chosen because they fulfill the recommended criteria with an RMSD of 0.725 Å (Figure 1). It was clear that the conformation of AMP before and after redocking was almost identical. AMP has a binding affinity of -7.35 kcal/mol and forms hydrogen bond interactions (H-bond) with residues Asp22 and Phe156 on the pyridine ring and Val49 and Ile131 on the phosphate groups of AMP. In addition, the AMP pyridine ring also exhibits hydrophobic interactions with Ile23. These results are in line with the study conducted by Michalska et al. [3].

Molecular docking of lig_C00013871 showed the most negative binding energy compared to native ligands and other analogs, which was -9.43 kcal/mol. In general, these quercetin derivatives exhibit the binding mode and Hbond on the hydroxy group of the benzene ring with Leu126, Ala134, and Ala154 (Figure 2a). Interestingly, this compound was able to interact

hydrophobically with Gly48 and Val49 which are conserved areas of ADPR.

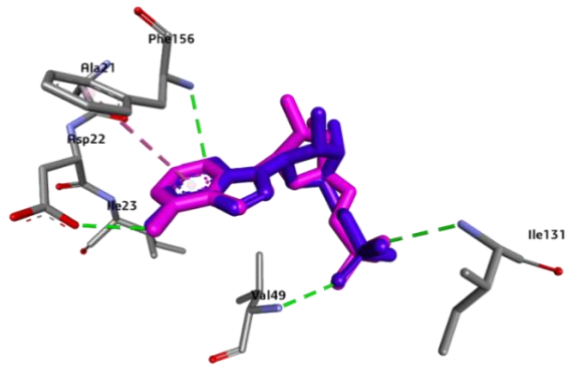

Figure 1. Overlay the 3D conformation of co-crystallized (pink) and docked AMP (blue) on the ADPR binding pocket of SARS CoV-2. Hydrogen bond and hydrophobic interactions were illustrated by green and pink dashed lines.

Interaction of Lig_C00006532 showed H-bond with several residues such as Ile23, Asn54, Lys55, and Ala154 (Figure 2b). This quercetin analog has a slightly positive binding energy compared to lig_C00013871 (-9.26 kcal/mol). Uniquely, the hydrophobic interaction with Phe156 on the adenine moiety between α2 and β7 strands of ADPR was observed on this analog.

On the other hand, lig_C00013874 has more positive binding energy than other analogs, namely -8.98 kcal/mol. Direct H-bond was observed around Leu126, Gly130, Gly133, and Ala154 in the main-chain amide of ADPR (Figure 2c). Uniquely, H-bond with Ala154 and Leu126 always appears in the two best quercetin analogs (lig_C00013871 and lig_C00013874). In addition, the hydrophobic interactions of lig_C00013874 and lig_C00013871 showed a similar trend with Gly48 and Val49 and formed new interactions with Gly130 and Val155.

a) lig_C00013871

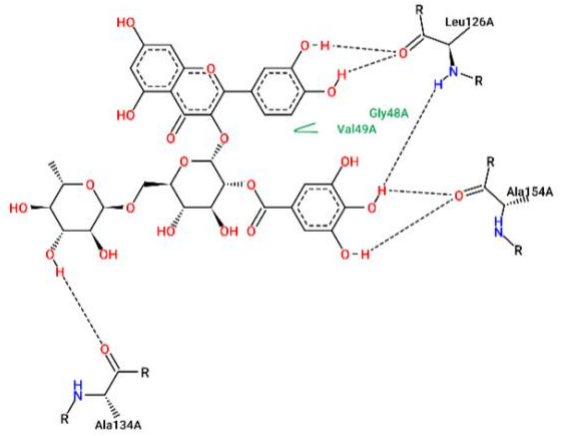

b) lig_C00006532

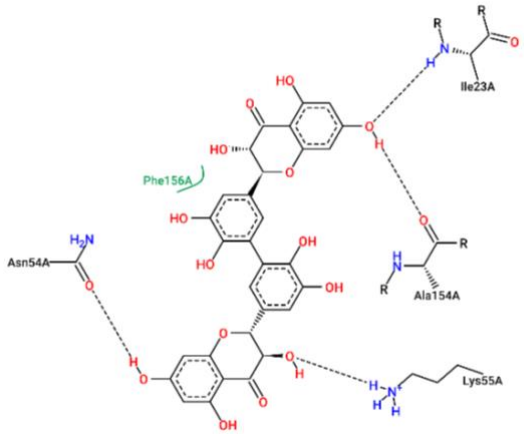

c) lig_C00013874

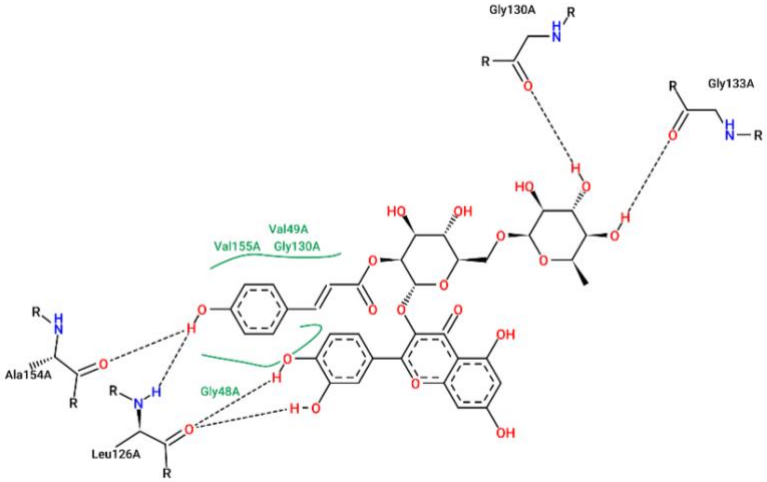

Figure 2. 2D interaction of a) lig_C00013871, b) lig_C00006532, and c) lig_C00013874 on the ADPR binding pocket of SARS CoV-2.

3.2 RMSD and RMSF Analysis

RMSD analysis of the ADPR system and the three best quercetin analogs (lig_C00006532, lig_C00013871, and lig_C00013874) are presented in Figure 3. The results showed that all complexes showed similar stability trends during 50 ns simulations with a maximum movement of 2.5 Å. Interestingly, the ADPR-AMP and ADPR-lig_C00013874 complexes had similar RMSD fluctuation with an average of 0.888 Å and 0.887 Å, respectively (Figure 3A and Figure 3D). In these two complexes at ~45 ns, the fluctuation decreased by ~0.5 Å and then increased to ~1.5 Å at the end of the simulation.

ADPR-lig_C00006532 and ADPR-lig_C00013871 systems showed the contrast trend of RMSD fluctuations. Complex lig_C00006532 had the highest fluctuation with an average of 0.893 Å, while lig_C00013871 tended to be more stable during the simulation, with the lowest changes of 0.839 Å (Figure 3B and Figure 3C).

We also analyzed the RMSD pattern of the quercetin analogs, which showed that all analogs showed similar fluctuations of ~0.5 Å, indicating satisfactory ligand stability during the simulation. The trend of AMP and lig_C00013871 was identical with increasing flux at ~30 ns, then stable until the end of the simulation. Lig_C00006532 showed sufficient stability, with the RMSD change occurring at ~10 ns increasing to ~1.25 Å, then decreasing to ~0.5 Å. Lig_C00013874 became the most stable analog by showing a constant movement trend (~0.5 Å) during simulation. RMSD analysis revealed the ability of the quercetin analog to stabilize the ADPR of SARS CoV-2 over a 50 ns simulation.

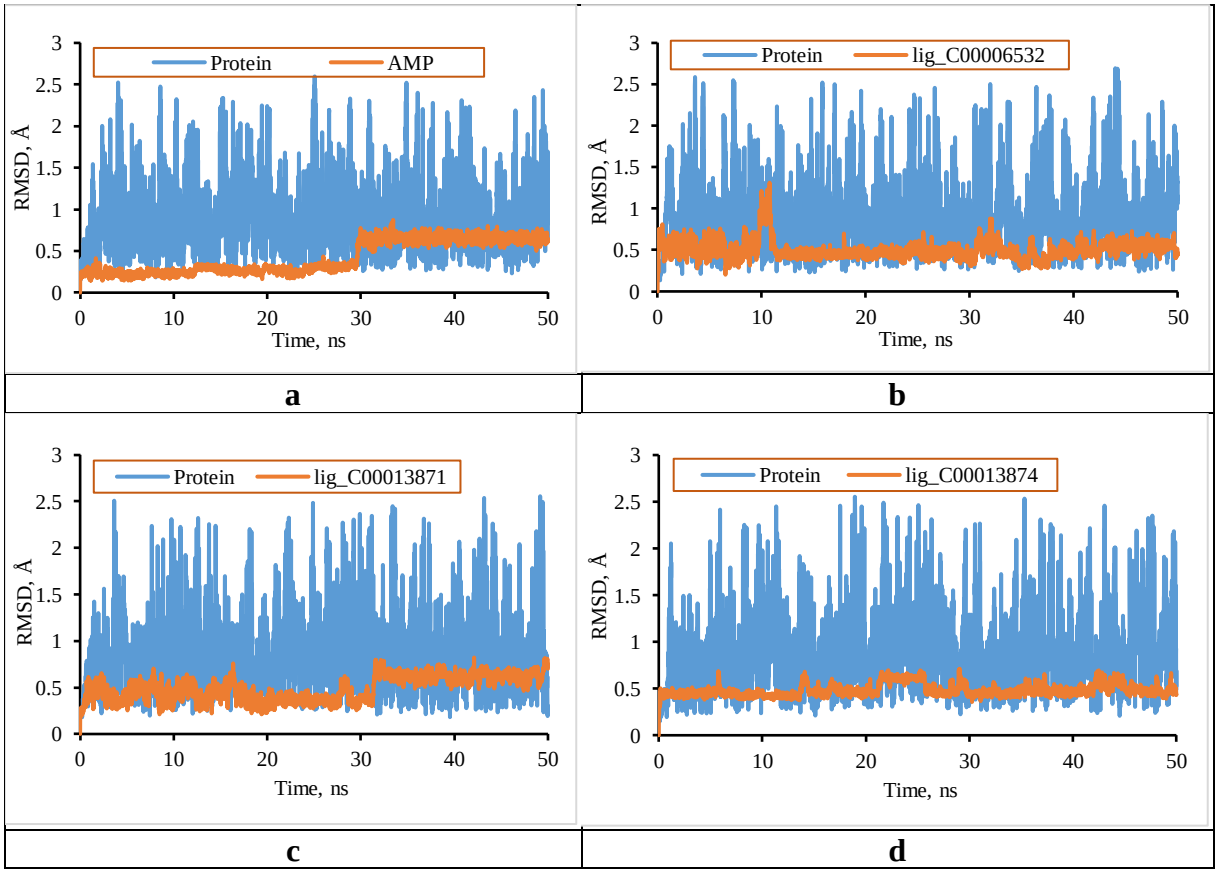

Figure 3. The root mean squared deviation (RMSD) of a) ADPR-AMP, b) ADPR-lig_C00006532, c) ADPR-lig_C00013871, and d) ADPR-lig_C00013874 systems. The RMSD of the ADPR backbone and ligands were shown in blue and orange lines, respectively.

RMSF was used to evaluate the stability of the ADPR residue during simulation. The RMSF of each system showed a similar fluctuations trend (Figure 4). It is plausible to conclude that three quercetin complexes appertained to the stable category with changes of less than 2 Å.

Fluctuations occurred in several residues, including Gly48, Asn87, Gly103, and Gly130, with oscillations of ~0.15 Å. Gly48 and Gly130 residues are conserved areas of ADPR pocket binding. In addition, the carboxyl (Val3) and amino (Glu170) end regions of ADPR showed

very high peak fluctuations at ~0.5 Å except for lig_C00013871. It was indicated that this residue has a high degree of structural disturbance.

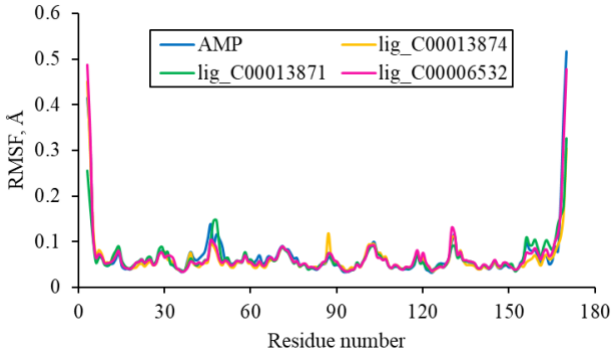

Figure 4. Root mean square fluctuation (RMSF) of the ADPR-AMP (blue), ADPR-lig_C00006532 (pink), ADPR-lig_C00013871 (green), and ADPR-lig_C00013874 (yellow) systems.

ADPR bound to lig_C00013874 caused the Asn87 residue to fluctuate slightly by 0.12 Å, while the other residues in the protein were stable. This fluctuation was not observed in other complex systems, so it is clear that quercetin analogs tend to stabilize ADPR and do not cause significant changes during simulation.

3.3 MM/GBSA Binding Energy Prediction

The MM/GBSA binding energy was calculated to assess the effectiveness of quercetin analogs for binding ADPR. The total binding energy (ΔE_{Bind}) for the AMP system was -14.76 kcal/mol, which was more positive than for the lig_C00006532 (-29.39 kcal/mol), lig_C00013871 (-34.90 kcal/mol) and lig_C00013874 (-42.79 kcal/mol) systems. Table 1 shows the calculated binding energies for the 50 ns of each system.

Table 1. The MM/GBSA binding free energy calculated for the AMP and quercetin analogs system.

Energy	AMP	A*	B*	C*
ΔE_{VDW}	-30.40	-42.95	-46.77	-58.08
ΔE_{ELE}	-86.72	-5.91	-13.67	-5.94
ΔE_{GB}	105.98	24.27	31.57	27.99
ΔE_{SURF}	-3.63	-4.80	-6.04	-6.76
ΔE_{Bind}	-14.76	-29.39	-34.90	-42.79

*A (lig_C00006532), B (lig_C00013871), and C (lig_C00013874).

It was observed that the van der Waals energy (ΔE_{VDW}) was the dominant factor when considering the contribution to the favorable binding energy, with -42.95 kcal/mol, -46.77 kcal/mol, and -58.08 kcal/mol, respectively, in lig_C00006532, lig_C00013871, and lig_C00013874. That energy was much more negative than the AMP system (-30.40 kcal/mol). A possible explanation was that the increased number of hydrophobic interactions of the quercetin analog with residues Gly48, Val49, Gly130, and Val155 appears to induce more favorable van der Waals interactions than AMP.

Electrostatic energy (ΔE_{ELE}) was more positive in the quercetin analogue system (-5.91 kcal/mol in lig_C00006532, -5.94 kcal/mol in lig_C00013874, and -13.67 kcal/mol in lig_C00013871), than in AMP (-86.72 kcal/mol). However, this was in contrast to the electrostatic contribution to the solvation energy (ΔE_{GB}), which was significantly more positive for AMP (105.98 kcal/mol) than the analogs lig_C00006532, lig_C00013874, and lig_C00013871 (24.27 kcal/mol, 27.99 kcal/mol, and 31.57 kcal/mol, respectively). Meanwhile, the non-polar contribution to the solvation energy (ΔE_{SURF}) had a favorable effect on the binding of the quercetin analog but did not change significantly during the simulation.

4 Conclusion

This study succeeded in identifying three quercetin analogs, lig_C00013871 (Quercetin 3-(2"-galoylrutinoside), lig_C00006532 ([5',5']-Bisdihydroquercetin), and lig_C00013874 (Quercetin 3-(2G-(E)-p-coumaroylrutinoside) which suspected to have ADPR inhibitory activity of SARS CoV-2. These three analogs have better affinity than AMP based on binding energy estimated from docking and MM/GBSA studies and and were capable of stabilizing the ADPR during molecular dynamics simulations. This research can be an impetus to prove these compounds' activity experimentally as inhibitors of ADPR.

Acknowledgement

This research was funded by Penelitian Dosen Pemula Internal UHO Tahun 2022, Institute for Research and Community Service, Universitas Halu Oleo, Kendari, Indonesia.

References

[[1] Adil MT, Rahman R, Whitelaw D, Jain V, Al-Taan O, Rashid F, et al. 2021. SARS-CoV-2 And The Pandemic Of COVID-19. *Postgrad Med J* 97(1144):110–6.

[2] Trougakos IP, Stamatelopoulos K, Terpos E, Tsitsilonis OE, Aivalioti E, Paraskevis D, et al. 2021. Insights To SARS-CoV-2 Life Cycle, Pathophysiology, And

Rationalized Treatments That Target COVID-19 Clinical Complications. *J Biomed Sci* 28(1):9.

[3] Michalska K, Kim Y, Jedrzejczak R, Maltseva NI, Stols L, Endres M, et al. 2020. Crystal Structures Of SARS-CoV-2 ADP-Ribose Phosphatase: From The Apo Form To Ligand Complexes. *IUCrJ* 7(5):814–24.

[4] Yadav R, Chaudhary JK, Jain N, Chaudhary PK, Khanra S, Dhamija P, et al. 2021. Role Of Structural And Non-Structural Proteins And Therapeutic Targets Of SARS-CoV-2 For COVID-19. Vol. 10, Cells .

[5] Armstrong LA, Lange SM, Dee Cesare V, Matthews SP, Nirujogi RS, Cole I, et al. 2021. Biochemical Characterization Of Protease Activity Of Nsp3 From SARS-CoV-2 And Its Inhibition By Nanobodies. *PLoS One* 16(7):e0253364.

[6] Mariano G, Farthing RJ, Lale-Farjat SLM, Bergeron JRC. 2020. Structural Characterization Of SARS-CoV-2: Where We Are, And Where We Need To Be. Vol. 7, Frontiers in Molecular Biosciences. p. 1–28.

[7] Lim CT, Tan KW, Wu M, Ulferts R, Armstrong LA, Ozono E, et al. 2021. Identifying SARS-CoV-2 Antiviral Compounds By Screening For Small Molecule Inhibitors Of Nsp3 Papain-Like Protease. *Biochem J* 478(13):2517–31.

[8] Leung AKL, McPherson RL, Griffin DE. 2018. Macrodomain ADP-Ribosylhydrolase And The Pathogenesis Of Infectious Diseases. *PLOS Pathog* 14(3):e1006864.

[9] Wyżewski Z, Gradowski M, Krysińska M, Dudkiewicz M, Pawłowski K. 2021. A Novel Predicted ADP-Ribosyltransferase-Like Family Conserved In Eukaryotic Evolution. *PeerJ* 9:e11051.

[10] Yan F, Gao F. 2021. An Overview Of Potential Inhibitors Targeting Non-Structural Proteins 3 (PL(Pro) And Mac1) And 5 (3CL(Pro)/M(Pro)) Of SARS-CoV-2. *Comput Struct Biotechnol J* 2021/08/24. 19:4868–83.

[11] Russo LC, Tomasin R, Matos IA, Manucci AC, Sowa ST, Dale K, et al. 2021. The SARS-CoV-2 Nsp3 Macrodomain Reverses PARP9/DTX3L-Dependent ADP-Ribosylation Induced By Interferon Signaling. *J Biol Chem* 297(3):101041.

[12] Jung LS, Gund TM, Narayan M. 2020. Comparison Of Binding Site Of Remdesivir And Its Metabolites With NSP12-NSP7-NSP8, And NSP3 Of SARS CoV-2 Virus And Alternative Potential Drugs For COVID-19 Treatment. *Protein J* 39(6):619–30.

[13] Debnath P, Debnath B, Bhaumik S, Debnath S. 2020. In Silico Identification Of Potential Inhibitors Of ADP-Ribose Phosphatase Of SARS-CoV-2 NsP3 By Combining E-Pharmacophore- And Receptor-Based Virtual Screening Of Database. *ChemistrySelect* 2020/08/11. 5(30):9388–98.

[14] Önal H, Arslan B, Üçüncü Ergun N, Topuz Ş, Yilmaz Semerci S, Kurnaz ME, et al. 2021. Treatment Of COVID-19 Patients With Quercetin: A Prospective, Single Center, Randomized, Controlled Trial. *Turkish J Biol = Turk Biyol Derg* 45(4):518–29.

[15] Agrawal PK, Agrawal C, Blunden G. 2020. Quercetin: Antiviral Significance And Possible COVID-19 Integrative Considerations. *Nat Prod Commun* 15(12):1–10.

[16] Di Pierro F, Iqtadar S, Khan A, Ullah Mumtaz S, Masud Chaudhry M, Bertuccioli A, et al. 2021. Potential Clinical Benefits Of Quercetin In The Early Stage Of COVID-19: Results Of A Second, Pilot, Randomized, Controlled And Open-Label Clinical Trial. *Int J Gen Med* 14:2807–16.

[17] Goris T, Pérez-Valero Á, Martínez I, Yi D, Fernández-Calleja L, San León D, et al. 2021. Repositioning Microbial Biotechnology Against COVID-19: The Case Of Microbial Production Of Flavonoids. *Microb Biotechnol* 2020/10/13. 14(1):94–110.

[18] Kim C-H. 2021. Anti–SARS-CoV-2 Natural Products As Potentially Therapeutic Agents . Vol. 12, Frontiers in Pharmacology .

[19] Morris GM, Huey R, Olson AJ. 2008. UNIT Using AutoDock For Ligand-Receptor Docking. Current Protocols in Bioinformatics.

[20] Li H, Leung K, Wong M. 2012. Idock: A Multithreaded Virtual Screening Tool For Flexible Ligand Docking. In: 2012 IEEE Symposium on Computational Intelligence in Bioinformatics and Computational

Biology (CIBCB) p. 77–84.

[21] Pronk S, Páll S, Schulz R, Larsson P, Bjelkmar P, Apostolov R, et al. 2013. GROMACS 4.5: A High-Throughput And Highly Parallel Open Source Molecular Simulation Toolkit. *Bioinformatics* 29(7):845–54.

[22] Petrov D, Zagrovic B. 2014. Are Current Atomistic Force Fields Accurate Enough To Study Proteins In Crowded Environments? *PLoS Comput Biol*.

[23] Wang J, Wolf RM, Caldwell JW, Kollman PA, Case DA. 2004. Development And Testing Of A General Amber Force Field. *J Comput Chem* 25(9):1157–74.

[24] Pearlman DA, Case DA, Caldwell JW, Ross WS, Cheatham TE, DeBolt S, et al. 1995. AMBER, A Package Of Computer Programs For Applying Molecular Mechanics, Normal Mode Analysis, Molecular Dynamics And Free Energy Calculations To Simulate The Structural And Energetic Properties Of Molecules. *Comput Phys Commun* 91(1):1–41.

[25] Sousa Da Silva AW, Vranken WF. 2012. ACPYPE - AnteChamber PYthon Parser InterfacE. *BMC Res Notes*.